Optimised genome editing for precise DNA insertion and substitution using Prime Editors in zebrafish

Yosuke Ono[1], Martin Peterka[2], Michael Love[3], Ashish Bhandari[1], Euan Gordon[2], Jonathan S. Ball[3], Charles R. Tyler[3], Steve Rees[4], Mohammad Bohlooly-Y[2], Marcello Maresca[2], and Steffen Scholpp[1*]

[1]Living Systems Institute, Biosciences, University of Exeter, United Kingdom; [2]Discovery Sciences, BioPharmaceuticals R&D, AstraZeneca, Gothenburg, Sweden; [3]Biosciences, University of Exeter, United Kingdom; [4]Discovery Sciences, BioPharmaceuticals R&D, AstraZeneca, Cambridge, United Kingdom

*Correspondence: s.scholpp@exeter.ac.uk

Abstract

CRISPR/Cas9-mediated genome editing has rapidly become a popular tool for studying gene functions and generating genetically modified organisms. However, using this system, stochastic integration of random insertions and deletions restricts precise genome manipulation. Advanced CRISPR/Cas9 technologies using Prime Editors (PEs), Cas9 proteins fused with reverse transcriptase, enable programmed integration of short DNA modifications into the genome. However, its application in precise genome editing in animal models is challenging. Here, we utilise a nickase- and a nuclease-based PE to perform programmed short DNA substitution and insertion in various loci in the zebrafish genome. Whereas the nickase-based PE is advantageous for nucleotide substitutions, we find that the nuclease-based PE can be used to insert short DNA fragments precisely with high efficiency. To further evaluate our approach, we inserted a nuclear localisation signal into a reporter transgene to incorporate longer fragments by prime editing. These gene modifications were transmitted to the next generation. We demonstrate that PE-mediated prime editing can efficiently manipulate genome information in zebrafish without using exogenous donor DNA.

Keywords

Prime editing, CRISPR/Cas9, zebrafish, PE2, PEn

Introduction

Genetically modified animals serve as powerful tools for studying ontogenesis and disease mechanisms in complex living systems. The zebrafish, *Danio rerio,* is a well-established model vertebrate species in cell and developmental biology due to attributes including its high fecundity in laboratory environments, transparency of the embryos, and amenability to the application of tools for transgenesis[1–3]. Zebrafish have also emerged as a powerful vertebrate model organism for studying human diseases, as they exhibit a substantial degree of genetic similarity with humans (around 70% of human genes having a corresponding gene in zebrafish)[4]. Several technologies for targeted mutagenesis, such as zinc finger nuclease (ZFN) and transcription activator-like effector nuclease (TALEN), have been employed in zebrafish to establish genetic loss-of-function mutants[5–8]. Most recently, CRISPR/Cas9-mediated genome editing has been introduced, significantly advancing target mutagenesis in nearly every model system, including zebrafish[9–13]. The CRISPR/Cas9 system has the potential to mimic disease phenotypes more accurately, allowing for the creation of identical genetic alterations corresponding to disease-causing mutations in humans. However, it has the disadvantage of stochastically generating insertions and deletions (so-called indels). This is because this technology relies on the DNA double-strand break (DSB) induced by the endonuclease at the target sequence in the genome and subsequent DNA repair. To allow precise control of genome editing, homology-directed repair (HDR)-mediated knock-in approaches using exogenous donor DNA have been utilised in zebrafish[14–16]. However, HDR-mediated precise genome editing occurs less efficiently compared with random mutagenesis.

Due to the need for precise genome editing with high efficiency, new strategies have been employed and applied in model organisms. For example, CRISPR/Cas9-mediated precise editing using Prime Editor has recently been developed, which does not rely on exogenous DNA donors. The original Prime Editor is a fusion protein of Cas9-nickase and reverse transcriptase[17]. By combining the Prime Editor with a prime editing guide RNA (pegRNA), the resulting Prime Editor ribonucleoprotein (RNP) complex generates a single-strand break (SSB) or nick at the target site in the genome. The reverse transcriptase domain elongates an additional DNA sequence at the 3’ end of cleaved DNA, following the reverse-transcription (RT) template sequence incorporated in the pegRNA. The additional short DNA fragment that contains the intended edit is integrated into the genomic DNA through the ligation of the 3’ flap and the excision of the competing 5’ flap from the original DNA sequence[17]. The

Cas9-nickase-based Prime Editor enables programmed short DNA modification (insertion, deletion and substitution), as has been shown in cultured cells, mouse and zebrafish embryos[17–20]. An alternative to the Cas9-nickase-based Prime Editor is prime editing with a Cas9-nuclease-based Prime Editor (PEn)[21–23]. PEn facilitates programmed short DNA modification through DNA repair based on homology annealing and non-homologous end joining (NHEJ) after DSB[22]. However, evidence for the successful use of Prime Editors in creating genetically modified animals is still limited. This is due to various technical challenges, including high variability in editing modes, low editing efficiency, and different delivery methods for prime editing components in living animals.

Here, we assess PE2, a nickase-based Prime Editor, and PEn-mediated prime editing for establishing genetically modified zebrafish for programmed DNA modification in their genome. We tested nucleotide substitution and the insertion of different lengths of DNA sequences, including a stop codon and nuclear localisation signal (NLS). We performed morphological assessments of these genetically modified embryos. We demonstrate that PE2-mediated prime editing is a favourable tool for base pair substitution in zebrafish embryos, whereas editing with PEn can more efficiently insert nucleotides up to 30 bp for modulating protein function and behaviour, all without using exogenous donor DNA. We further show that stable genetically modified zebrafish lines can be generated that inherit these programmed short DNA modifications.

Results

Prime editing in nucleotide substitution

First, we tested the use of Prime Editors for substituting specific base pairs in the zebrafish genome. To do this, we focused on the Cereblon (CRBN) gene, which has been associated with developing resistance to thalidomide-based treatments, particularly in conditions like multiple myeloma[24,25]. Here, we first compared the functioning of nuclease-based PEn and nickase-based PE2 in nucleotide substitution in the zebrafish *crbn* gene (Fig. 1a), targeting the sequence encoding the amino acid residue I378 associated with the sensitivity to thalidomide and related drugs[26,27]. A mixture of Prime Editor proteins and chemically synthesised pegRNAs for substituting 2 single nucleotides in the target sequence (+3 G to C and +10 A to G; Supplementary Fig. 1a) was injected into zebrafish embryos at the early 1-cell stage, after which the embryos were incubated at 32°C. Genomic DNA was then

extracted from these embryos at 96 hours post-fertilisation (hpf) to analyse genome edits at the target site. Amplicon sequencing of the target region showed that both PEn and PE2 integrated the prime editing substitution into the genome (Fig. 1b). We found that PE2 had a higher efficiency in precise substitutions (8.4%) compared to PEn (4.4%, Fig. 1c). Furthermore, PEn induced a higher amount of indels (Fig. 1d). The precision score, defined as the ratio of precise prime edits to the total edits, including imprecise prime edits and indels, was significantly higher with PE2 (40.8%) compared to PEn (11.4%, Supplementary Fig. 1b). We also tested the refolding procedure of pegRNA to prevent misfolding between the complementary sequences in the spacer sequence and primer binding site (PBS) and RT template sequence[28]. Refolding of the *crbn* pegRNA did not enhance prime editing substitution with both PEn and PE2 (Fig. 1c). These results indicate that PE2 is the more effective for very short nucleotide substitution compared with PEn in zebrafish.

Prime editing insertion of 3 bp DNA fragment

Next, we tested the functioning of the Prime Editors in the precise insertion of a 3 bp stop codon into the coding sequence of the endogenous target gene to generate a mutant allele that produces a precisely truncated protein. As a proof-of-concept, we chose the cognate receptor gene *ror2*. Genetic mutations in the *ROR2* gene in humans can cause the autosomal recessive Robinow syndrome, leading to short stature, distinctive facial features, and skeletal abnormalities, including short limbs and a curved spine (*scoliosis*)[29–31]. In zebrafish, the inhibition of Ror2 signalling function affects the convergence and extension of axial cells during gastrulation and the elongation of the embryo body, leading to a broader and shorter body axis[32–35], as well as the patterning of cranial tissues[36], and thus would be an excellent model for studying many aspects of the Robinow syndrome.

Sequence comparison suggested that the zebrafish W722X allele corresponds to the human disease-related W720X mutation generating a premature stop codon (TGA) in the tyrosine kinase domain (Fig. 2a). Therefore, we aimed to establish the zebrafish Robinow W722X model by designing pegRNA and single primed insertion gRNA (springRNA)[22] generating a similar stop codon into the sequence of exon 9 in zebrafish *ror2*. The pegRNA contained a 3 nt RT template sequence for the stop codon to be integrated, 13 nt PBS sequence, and 13 nt sequence to extend the homology arm for the DNA integration via homology annealing (Fig. 2b and c). We compared this strategy to using a springRNA

combined with PEn, without the template sequence for the homology arm, to insert the stop codon via NHEJ (Fig. 2b and c). We microinjected combinations of Prime Editor mRNA and guide RNA, that is, PE2/pegRNA, PEn/pegRNA and PEn/springRNA at the one-cell stage in zebrafish embryos. The sequence in *ror2* exon 9 was amplified by PCR from a pool of genomic DNA obtained from 10 injected embryos, and the induction of DNA modification was assessed by a T7 endonuclease I (T7E1) assay. We observed the cleavage of PCR products in the samples injected with PEn/pegRNA and PEn/springRNA combinations, indicating sequence modification in the target site (Fig. 2d). In contrast to the base pair substitution, PE2 was less effective.

The PCR products were also cloned into a cloning vector, and the target sequences in randomly selected clones were analysed. Various types of edits in the target site were observed in the clones from the PEn injected samples, including precise insertion of the stop codon and/or random indels (Fig. 2e), although no sequence edits in the target site were identified from the PE2 injected sample (0/20 clones; Supplementary Fig. 2). Subsequently, we performed amplicon sequencing to quantify the proportion of each genome edit. We found that the proportion of precise prime editing (only TGA insertion without any indels) was higher when using PEn/pegRNA combination (10.3%) compared to PEn/springRNA (4.0%) and PE2/pegRNA (0.4%, Fig. 2f). In addition, springRNA showed a higher proportion of imprecise prime edit (TGA insertion with random indels; 37.5%) than pegRNA (11.1% and 0.2% with PEn and PE2, respectively; Fig. 2f). The precision scores for the PE2/pegRNA, PEn/pegRNA, and PEn/springRNA combinations were 58.9%, 32.6%, and 7.8%, respectively. This suggests that prime editing via homology annealing with pegRNA was more accurate than via NHEJ using springRNA.

Comparison of the mode of Prime Editor delivery as mRNA or RNP complex

Next, we compared PEn and PE2 in combination with different strategies of Prime Editor delivery. Here, we performed amplicon sequencing with genomic DNAs extracted from individual embryos injected with Prime Editor mRNA or RNP complex with the *ror2* pegRNA (Fig. 3a). We found that the proportion of precise prime edit is significantly increased with PE2 RNP complex (11.5%) compared to PE2 mRNA (1.3%), whereas the there is no significant difference between PEn RNP complex (20.5%) compared to PEn mRNA (18.8%; Fig. 3b). However, with both delivery methods of the Prime Editors, the

proportion of precise prime edit was significantly higher with PEn compared to PE2, supporting our previous results (Fig. 2f and 3b). Furthermore, PEn also integrated a notably higher number of indels that are unrelated to prime editing (Fig. 3c), resulting in lower precision scores with PEn (34.3% and 28.2% for mRNA and RNP delivery, respectively) compared to PE2 (71.6% and 43.4% for mRNA and RNP delivery, respectively; Supplementary Fig. 3a). These findings suggest that the PEn-induced DNA DSBs are more like to undergo repair events (both precise and imprecise) compared to the nickase-based PE2 method.

Induction of abasic spacer into springRNA to prevent gRNA scaffold insertion

In the analysis of the sequence edits in the *ror2* gene by PEn-mediated prime editing, we found that a substantial proportion of the amplicons derived from embryos injected with the PEn/springRNA combination contained imprecise prime edits with additional nucleotides that correspond to the sequence of gRNA scaffold adjacent to the RT template (Fig. 3d and Supplementary Fig. 3d), as reported previously[18]. This finding suggests that the readthrough of RT from the template sequence into the gRNA scaffold causes unintended insertions, as has also been reported in human cell lines[17,37]. Aiming to control the termination of RT in prime editing, we synthesised a modified springRNA in which an abasic RNA spacer was inserted between the RT template and gRNA scaffold (Fig. 3e). Microinjection of the abasic springRNA together with PEn mRNA or RNP complex significantly reduced the unintended insertion of gRNA scaffold sequence into the target site (Fig. 3f). However, the proportion of precise prime edits did not show a significant improvement (Fig. 3g). Due to the significantly reduced number of the imprecise prime edits, the precision scores increased from 9.6% to 21.7% and from 10.6% to 14.2% with PEn mRNA and RNP complex, respectively, through the blocking of scaffold sequence incorporation (Supplementary Fig. 3b). These results suggest that the read-through process is independent of precise genome editing events in zebrafish embryos, unlike in human cultured cells[37].

Prime editing in adgrf3b gene using PEn

Next, we tested the PEn-mediated prime editing targeting at a different locus, here the *adgrf3b* gene. A previously published study has reported that the efficiency of prime editing

in the *adgrf3b* gene using PE2 and pegRNA was decreased from 18.0% to 0.1% by extending the length of prime editing insertion from 3 bp to 12 bp[18]. Therefore, we tested the efficiency of our nuclease-based PE by injecting PEn mRNA with pegRNA or springRNA targeting the same sequence in the *adgrf3b* gene to integrate the 3 bp or 12 bp insertion. Both PEn/pegRNA and PEn/springRNA combinations successfully integrated the programmed 3 bp and 12 bp insertion into the target site in the injected embryos. Here, the mean proportion of precise prime edit with pegRNA and springRNA in amplicon sequencing was 27.3% and 4.0% for 3 bp insertion and 1.9% and 0.7% for 12 bp insertion, respectively (Fig. 3h and i). The precision scores with pegRNA and springRNA were 42.1% and 4.6% for a 3 bp insertion and 8.6% and 1.1% for a 12 bp insertion, respectively (Supplementary Figure 3c), suggesting that both the efficiency and accuracy of prime editing declined with an increase in insertion length. Both PEn/pegRNA and PEn/springRNA combinations performed more efficiently with the 12 bp insertion compared to that reported previously using the PE2 system, this suggests that PEn-generated DNA DSB accepts longer insertion than a nickase-based Prime Editor in zebrafish embryos.

Establishing stable ror2^{W722X} mutant zebrafish

Having demonstrated the programmed insertion via PEn-mediated prime editing in injected embryos, we wanted to establish if these precise edits are passed on to the next generation, as this is a prerequisite for establishing a disease model. We, therefore, aimed to develop stable *ror2*^{W722X} mutant zebrafish. Therefore, first, we injected embryos with PEn RNP complex and the *ror2* springRNA and raised the embryos to adults, and then we outcrossed them with wild-type fish to collect F1 embryos. Through genotyping 16 embryos from each F0 adult fish, we obtained F1 embryos harbouring the *ror2*^{W722X} mutation. Six out of 10 F0 adults were founders of the allele, with the germline transmission rate varying between 6.3% (1/16) and 31.3% (5/16; Fig. 4a). We raised the F1 heterozygous *ror2*^{W722X} fish and inbred them to generate homozygous *ror2*^{W722X} mutant embryos in the F2 generation. The morphology of the zygotic *ror2*^{W722X} mutant embryo and larvae was similar to wild-type siblings, and the mutant animals were both viable and fertile (Fig. 4b, c and e). Subsequently, we generated maternal-zygotic (MZ) mutants by in-crossing homozygous *ror2*^{W722X} male and female fish. The MZ *ror2*^{W722X} mutant larvae at 5 dpf showed a mild curvature of the tail tip and shorter body length (Fig. 4d and f), which are similar phenotypes to the MZ mutant

larvae of the loss-of-function alleles in *ror2* reported previously[32,36]. This suggests that the human disease-related *ror2*^{W722X} mutation in the tyrosine kinase domain affected the Wnt/PCP signalling similarly to the observation in patients with Robinow syndrome. This set of data suggests that PEn-based editing can be used to establish stable genetically modified fish lines.

Insertion of nuclear localisation signal into transgenic reporter gene

After the successful insertion of the 3 bp stop codon into the *ror2* gene to establish a zebrafish model of the Robinow syndrome and successful 3 and 12 bp insertions into the *adgrf3b* gene, we tested whether PEn-mediated prime editing can be used to integrate up to 30 bp. Since we anticipated that these events would be rare, we employed a strategy that enabled us to screen for prime edit events and distinguish between imprecise prime edits and random indels at the cellular level in living zebrafish embryos, all without the need for time-consuming sorting and genetic analysis. This was achieved using an eGFP-transgenic fish line with an introduced nuclear localisation sequence (NLS) of 27 bp using PEn. We anticipated three phenotypes: cytosolic GFP localisation for unsuccessful editing, no GFP expression for imprecise edits, and nuclear GFP expression for precise prime editing insertion (Fig. 5a). We subsequently mapped these effects in individual cells using high-resolution confocal microscopy in living zebrafish larvae. Specifically, we tested the insertion of the NLS sequence into the *smyhc1:gfp* transgene by prime editing. The *smyhc1:gfp* reporter gene is expressed explicitly in the superficial slow-twitch muscle fibres in the body trunk (Supplementary Fig. 4a), which are mononuclear during embryonic development[38]. We designed pegRNAs that target the N-terminal end of the eGFP coding sequence in the *smyhc1:gfp*^{i104} transgenic allele and contain RT template sequence for inserting c-myc NLS[39–41]. We expected that precise integration of the 30 bp sequence, including 27 bp c-myc NLS and 3 bp spacer, translocates the eGFP expression from the cytoplasm to the nucleus in the muscle fibres, whereas reporter expression is lost in the cells with imprecise prime edits or random indels by frameshifting in the eGFP coding sequence (Fig. 5a). The embryos injected with PEn RNP complex showed mosaic expression of eGFP in the cytoplasm of muscle fibres, lack of GFP expression in some fibres along with the accumulation of eGFP signals in a few cell nuclei (Fig. 5b). Amplicon sequencing of the target region in the genome showed that the average efficiency of precise prime editing insertion in the whole injected

embryo was 8.5% with a precision score of 9.7% (Fig. 5c). We also compared the prime editing efficiency to that using a longer pegRNA in which PBS sequence and template sequence of the homology arms were extended from 10 nt to 13 nt and 14 nt to 36 nt, respectively. However, the prime editing efficiency of the longer pegRNA was significantly decreased, possibly due to increased RNA complexity leading to altered secondary structures (Fig. 5c).

Next, to establish stable genetically modified zebrafish lines with the NLS insertion, we raised F0 injected fish to adults, outcrossed them with wild-type, and screened the F1 embryos for their GFP expression. We successfully isolated embryos showing pronounced eGFP expression in the nuclei of slow-twitch fibres (Fig. 5d and Supplementary Fig. 4b). We confirmed the integration of the 30 bp sequence into the eGFP coding sequence (Fig. 5e and Supplementary Fig. 4c). Notably, multiple types of edits were also identified in the amplicons obtained from the single embryo with nuclear eGFP expression, suggesting that the *smyhc1:gfp*^{i104} transgenic allele contains at least 4 copies in this locus. Each copy was targeted and edited individually by PEn/pegRNA complex (Fig. 5e and Supplementary Fig. 4c). Here, 4 F0 adult fish out of 6 screened were identified as founder fish of the prime editing insertion in the target transgene. The proportion of the embryos showing nuclear eGFP expression varied between 1.4 to 20.2% (Fig. 5f). Our findings indicate that PEn-mediated precise DNA insertion is a practical tool for the accurate integration of functional motifs with a length of up to 30 bp within a target gene in zebrafish.

Discussion

The need for precise genome editing

Target sequence-specific mutagenesis and transgenesis are essential tools for analysing gene functions, and labelling expressed proteins, cellular components and specific cell types *in vivo*. Induction of DSB in the genome DNA by ZFN, TALEN and CRISPR/Cas9 technologies enable random mutagenesis and donor DNA-based knock-in in the target sequence. In addition to the conventional HDR-mediated knock-in, multiple systems for targeted integration into the genome in zebrafish have been reported[42,43]. Adding further to this, Cas9-nickase fusion proteins with cytidine or adenine deaminase, so-called Base Editors[44,45], enable single nucleotide substitution in zebrafish to generate human disease models[46–51]. Despite advancements in gene editing technologies, however, the application of

Prime Editors for the generation of genetically modified animals remains restricted[18,52,53]. This limitation can be attributed to several technical hurdles, including substantial variability in editing modes, suboptimal editing efficiency, and complications associated with the delivery of prime editing components *in vivo*.

In this study, we established programmed short DNA modification in the genome using Prime Editors and generated stable genetically modified zebrafish lines with 3 and 30 bp insertions. Firstly, we utilised PE2 for successful nucleotide substitution in a target sequence associated with drug sensitivity and PEn to generate a zebrafish model for human genetic disease. Specifically, we established a stable *ror2*^{W722X} mutant line, which genocopies the disease-related W720X mutation in the human *ROR2* gene. Various mutations have been identified in the human *ROR2* gene as the causes of Robinow syndrome, and different types of mutation lead to distinct phenotypes and inheritance patterns, possibly due to nonsense-mediated decay of mutated mRNA[54], the mechanism which is also essential for embryonic development and tissue homeostasis in zebrafish[55,56]. Establishing genetically modified zebrafish carrying mutations related to genetic disease in humans will enable a more precise analysis of the mechanisms of genetic diseases. Using prime editing and base editing by Base Editors will open a wider window for precise genome editing in zebrafish for both drug discovery and human disease models.

Secondly, we inserted a functional motif in existing lines to control the features of a protein. Here, specifically, we inserted an NLS sequence into the *smyhc1:gfp*^{i104} transgene and assessed the prime editing *in vivo* by translocating eGFP expression. The same approach can be applied to tag endogenous proteins and control their localisation and transport. The pegRNAs we used to insert NLS were designed in the coding sequence of the N-terminal region of eGFP, and therefore, the strategy can be used for other established eGFP reporter zebrafish lines to convert their GFP expression from the cytoplasm to the cell nuclei and as a control to assess prime editing *in vivo* morphologically.

Previous studies have reported a low efficiency of prime editing insertion. In those studies it is proposed that the length negatively correlates with prime editing efficiency, while the MLH1 protein influences editing outcomes for short sequences up to 13 bp in cultured cells[57–59]. Enhancing pegRNA stability and preventing degradation can further improve editing efficiency[28,60,61]. Finally, co-expressing effector proteins with Prime Editor to

suppress undesired DNA repair pathways or protect pegRNA from degradation has been suggested to enhance editing[23,58,62].

The underlying mechanism of PEn-mediated precise genome editing

Here, we demonstrated that a nuclease-based PE can efficiently integrate DNA insertions between 3–30 bp in zebrafish embryos. By utilising pegRNA and springRNA, we show that the integration is based on both homology annealing and NHEJ, as suggested in cell culture[22]. Although pegRNA was superior to springRNA in both efficiency and accuracy at the tested target loci, springRNA could be advantageous when longer PBS and/or RT template sequences are necessary, as it lacks a template for homology arms. We also observe that the repair outcome varies depending on the delivery mode of the PEn. Microinjection of PEn mRNA leads to fewer indels than supplying the PEn as an RNP complex, although there was no significant difference in the level of precise prime edit (Fig. 3). We hypothesise that the RNP complex acts faster than the mRNA and a potential explanation could be that the relatively rapid integration of random indels is more effective than the prime editing reaction in the early zebrafish embryo (0–3 hpf), when cell cycle time is significantly shorter (approximately 25 min). However, the precise DNA repair mechanism and accessibility to a target site in the genome for the prime editing reaction in relation to the cell cycle duration need to be explored in the future.

We also show that nuclease-based PE has its limitations. For example, we found that the nickase-based PE2 seems to be a favourable tool for nucleotide substitution, as shown for *crbn* (Fig. 1). Further analyses will be required to compare nuclease-based and nickase-based Prime Editors, focusing on the distance between the substitution sites and Cas9 nicking/cleavage site. Furthermore, as PEn functions via DSB of genomic DNA, insertion can potentially cause off-target effects, large deletions, and chromosomal rearrangements[63–65], whereas the level of large deletions in PEn-mediated prime editing is comparable to that with the nickase-based PE2 in cultured cells[22]. It will be interesting to see whether these adverse effects that occurred in injected zebrafish can be neutralised by outcrossing against wild-type fish in the next generations.

In conclusion, we have established genetically modified zebrafish with programmed short DNA modifications by microinjecting PE mRNA or RNP complex with gRNAs that integrate DNA modification via different DNA repairing pathways. Prime editing insertions were

germline-transmitted to the next generation with high efficiency to establish stable genetically modified zebrafish lines. Our PE-mediated insertion method in zebrafish embryos offers a highly efficient, low-error approach for editing the genome *in vivo*. The method can be employed to manipulate coding sequences in endogenous genes and to insert functional DNA motifs for protein tagging and modulating gene expression. Thus, the findings suggest broad applicability for Prime Editors across model organisms by offering donor DNA-free precise gene editing capabilities.

Materials and Methods

Zebrafish strains and husbandry

Wild-type zebrafish strains WIK and AB and the *Tg(smyhc1:gfp)*^{i104} transgenic line[38] were used to provide embryos. The collected embryos were raised at 28°C. Adult fish stocks were reared and maintained in the Aquatic Resources Centre at the University of Exeter under the conditions stated in the previous study[66]. The experimental procedures involving the animals were reviewed and approved by the United Kingdom Home Office under the Animals Scientific Procedures Act 1986 (project license: PP3975835) and received ethical approval from the Animal Welfare and Ethical Review Body at the University of Exeter.

Preparation of pegRNA and springRNA

The sequences of the pegRNA and springRNA for prime editing in the *ror2* and *crbn* genes, and for the *smyhc1:gfp* transgene, are listed in Supplementary Table 1. The pegRNAs for prime editing insertion in the *adgrf3b* gene have been reported in a previous study[18]. The first three nucleotides and inter-nucleotide linkages at both ends of the gRNA were chemically modified with 2'-O-methylation and phosphorothioate, respectively. Chemically modified synthetic gRNAs were obtained from Integrated DNA Technologies. The *ror2* springRNA with an abasic RNA spacer was sourced from Horizon Discovery. Synthesised gRNAs were dissolved in nuclease-free duplex buffer (Integrated DNA Technologies) at 100 µM and stored at −20°C.

Microinjection

Microinjection into one-cell stage embryos was carried out under a stereomicroscope using a FemtoJet 4x microinjector (Eppendorf). To prepare an injection mixture for prime editing, 1.25 µl of 600 ng/µl Prime Editor mRNA or 0.6 µl of 10 mg/ml purified Prime Editor protein was combined with 2.5 µl of 12 µM gRNA and 0.5 µl of 0.5% phenol red (Sigma), and the volume was adjusted to 5 µl with 2 M potassium chloride. PEn and PE2 mRNA were synthesised from the linearised plasmids[22] using the mMESSAGE mMACHINE T7 kit (Invitrogen), following the manufacturer's instructions. Purified Prime Editor proteins were prepared according to the protocol in the previous study[37]. A mixture of Prime Editor protein

and gRNA was incubated at 37°C for 5 minutes prior to microinjection to form an RNP complex. Glass needles for microinjection were prepared from glass capillaries (TW100F-4, World Precision Instruments) using a P-1000 micropipette puller (Sutter Instrument). Approximately 1–1.7 nl of the injection mixture was injected per embryo. After microinjection, the injected embryos were incubated in E3 embryo medium (5 mM sodium chloride, 0.17 mM potassium chloride, 0.33 mM calcium chloride, and 0.4 mM magnesium chloride; pH 7.2) at 32°C, following the protocol by Petri et al[18].

DNA extraction, PCR analyses and molecular cloning

Genomic DNA was extracted from individual embryos and larvae using the modified HotSHOT method[67]. The target region for prime editing in *ror2*, *adgrf3b*, and *smyhc1:gfp* was amplified by PCR using the following primer sets: *ror2* (5'-AAACTTATGGGTGCCAGTCC-3' and 5'-ATGGACACAAACTGAGGCTG-3'), *adgrf3b* (5'-TGATTGCATACACACCTGACC-3' and 5'-AGGCACCTGCAGGAAAATTA-3'), and *smyhc1:gfp* (5'-TGCAGTTACAAGGTACAGAGGTC-3' and 5'-CGTCCTTGAAGAAGATGGTGCG-3'). The PCR mixture was prepared as follows: 10 µl of 2x PCRBIO Taq Mix red (PCR Biosystems), 0.8 µl each of 10 µM forward and reverse primers, 1 µl of genomic DNA pooled from 10 individual samples, and 7.4 µl of water, totalling a volume of 20 µl. The PCR settings were as follows: 95°C for 1 min; 28 cycles of 95°C for 15 s, 58°C for 15 s, and 72°C for 15 s, followed by 72°C for 1 min. The mutation in the target sequence of the PCR product was assessed by the T7 endonuclease I (T7E1) assay. PCR products were denatured at 95°C for 5 min and then cooled to room temperature to form heteroduplex DNAs. Subsequently, 5 µl of PCR product was mixed with 1 µl of NEBuffer 2 (New England Biolabs), 0.15 µl of T7E1 enzyme (10 U/µl, New England Biolabs), and 3.85 µl of water to a total volume of 10 µl and incubated at 37°C for 15 min. The PCR and T7E1-digested products were assessed on a 3% agarose gel alongside a 100 bp DNA ladder (New England Biolabs). PCR products were also cloned into the pGEM-T Easy vector (Promega) and used for transformation with One Shot TOP10 chemically competent cells (Invitrogen) following the manufacturer's instructions. Bacterial colonies grown on an LB agar plate with 100 µg/ml ampicillin were randomly selected and used for plasmid extraction using a GeneJET plasmid miniprep kit (Thermo Scientific). Sanger sequencing of PCR products and plasmids was performed by Eurofins Genomics.

Amplicon sequencing and bioinformatics

PCR amplicons for next-generation sequencing (NGS) of *ror2*, *adgrf3b*, *crbn*, and *smyhc1:gfp* were prepared using Phusion Flash High-Fidelity 2x Mastermix (F548, Thermo Scientific) in a reaction volume of 15 µl, which contained 1.5 µl of genomic DNA extract and 0.2 µM of specific primers with barcodes and adapters for NGS. All primer sequences are shown in Supplementary Table 2. The PCR protocol with Phusion Flash High-Fidelity 2x Mastermix included an initial step at 98°C for 3 min, followed by 30 cycles at 98°C for 10 s, 60°C for 5 s, and 72°C for 5 s. The resulting PCR amplicons were purified using the HighPrep PCR Clean-up System (MagBio Genomics). The characterisations of size, purity, and concentration of the amplicons were conducted using a fragment analyser (Agilent). A second PCR was carried out to add Illumina indexes to the amplicons, utilising KAPA HiFi HotStart Ready Mix (Roche) in a total volume of 25 µl, containing 0.067 ng of PCR template and 0.5 µM indexed primers (Illumina). The PCR conditions were set at 72°C for 3 min, 98°C for 30 s, followed by 10 cycles at 98°C for 10 s, 63°C for 30 s, and 72°C for 3 min, with a 5-minute final extension at 72°C. Amplicons were purified with the HighPrep PCR Clean-up System (MagBio Genomics) and analysed using a fragment analyser (Agilent). Quantification was performed using a Qubit 4 Fluorometer (Life Technologies), with sequencing carried out on the Illumina NextSeq system in accordance with the manufacturer's guidelines. Demultiplexing of the amplicon sequencing data was executed with bcl2fastq software. The resulting fastq files were processed with CRISPResso2 V2.2.12 in prime editing mode[68]. Detailed parameters of the CRISPResso analysis can be found in Supplementary Table 3.

Live imaging

Stereomicroscope images were obtained using an Olympus DP73 microscope camera, and measurements were conducted with cellSens imaging software (Olympus). Confocal images of *smyhc1:gfp* transgene expression were captured with a Leica TCS SP8 laser scanning microscope using a HC Fluotar L 25×/0.95 water objective and LAS X imaging software (Leica). For imaging, live zebrafish larvae were affixed to glass slides with 1% low melting agarose (5806A, Takara) in an E3 embryo medium containing 200 µg/ml tricaine (A5040, Sigma).

Statistics

Data visualisation and statistical analyses were conducted using GraphPad Prism 10.4 (GraphPad Software), BioRender Graph (R version 4.2.2), and Adobe Illustrator. For statistical analysis, the numerical dataset from each experimental condition was examined using the Shapiro-Wilk test for normality and Levene's test for homogeneity of variance. One-way ANOVA with Tukey multiple comparison test, Welch's one-way ANOVA with Dunnett T3 multiple comparison test (parametric), or Kruskal-Wallis test with Dunn's multiple comparison test (nonparametric) was utilised to assess differences between three or more groups. The Mann-Whitney U test (nonparametric) was employed to evaluate differences between the two groups. The sample size for each experiment is presented in the figures and legends.

Acknowledgements

Research in the S.S. lab, including Y.O. and A.B., is supported by the Biotechnology and Biological Sciences Research Council Industrial Partnership Awards with AstraZeneca (BBSRC-IPA, BB/X008401/1; awarded to S.S., Y.O., and C.R.T) and the Living Systems Institute Open Innovation Platform Fund at the University of Exeter (awarded to Y.O.). M.L. receives support from the National Centre for the Replacement, Refinement and Reduction of Animals in Research (NC3Rs) PhD studentship (NC/X001407/1; awarded to J.S.B and C.R.T). We thank the Aquatic Resources Centre at the University of Exeter for the care of zebrafish resources.

Author contributions

Y.O., M.P., M.M., and S.S. conceived the study and designed the experimental strategy. Y.O., M.L., and A.B. performed the animal experiments and Y.O. and M.P. analysed the data with support from E.G., J.S.B., C.R.T., S.R., and M.B. The manuscript was prepared by Y.O. and S.S.

Competing interests

M.P., E.G., S.R., M.B., and M.M. are employees of AstraZeneca and may be AstraZeneca shareholders.

References

1. Kwan, K. M. et al. The Tol2kit: a multisite gateway-based construction kit for Tol2 transposon transgenesis constructs. *Dev. Dyn.* **236**, 3088–3099 (2007). 10.1002/dvdy.21343.

2. Grabher, C., Joly, J. S. & Wittbrodt, J. Highly efficient zebrafish transgenesis mediated by the meganuclease I-SceI. *Methods Cell Biol.* **77**, 381–401 (2004). 10.1016/s0091-679x(04)77021-1.

3. Thermes, V. et al. I-SceI meganuclease mediates highly efficient transgenesis in fish. *Mech. Dev.* **118**, 91–98 (2002). 10.1016/s0925-4773(02)00218-6.

4. Patton, E. E., Zon, L. I. & Langenau, D. M. Zebrafish disease models in drug discovery: from preclinical modelling to clinical trials. *Nat. Rev. Drug Discov.* **20**, 611–628 (2021). 10.1038/s41573-021-00210-8.

5. Meng, X., Noyes, M. B., Zhu, L. J., Lawson, N. D. & Wolfe, S. A. Targeted gene inactivation in zebrafish using engineered zinc-finger nucleases. *Nat. Biotechnol.* **26**, 695–701 (2008). 10.1038/nbt1398.

6. Doyon, Y. et al. Heritable targeted gene disruption in zebrafish using designed zinc-finger nucleases. *Nat. Biotechnol.* **26**, 702–708 (2008). 10.1038/nbt1409.

7. Huang, P. et al. Heritable gene targeting in zebrafish using customized TALENs. *Nat. Biotechnol.* **29**, 699–700 (2011). 10.1038/nbt.1939.

8. Sander, J. D. et al. Targeted gene disruption in somatic zebrafish cells using engineered TALENs. *Nat. Biotechnol.* **29**, 697–698 (2011). 10.1038/nbt.1934.

9. Varshney, G. K. et al. High-throughput gene targeting and phenotyping in zebrafish using CRISPR/Cas9. *Genome Res.* **25**, 1030–1042 (2015). 10.1101/gr.186379.114.

10. Jao, L. E., Wente, S. R. & Chen, W. Efficient multiplex biallelic zebrafish genome editing using a CRISPR nuclease system. *Proc. Natl. Acad. Sci. USA.* **110**, 13904–13909 (2013). 10.1073/pnas.1308335110.

11. Hwang, W. Y. et al. Efficient genome editing in zebrafish using a CRISPR-Cas system. *Nat. Biotechnol.* **31**, 227–229 (2013). 10.1038/nbt.2501.

12. Burger, A. et al. Maximizing mutagenesis with solubilized CRISPR-Cas9 ribonucleoprotein complexes. *Development* **143**, 2025–2037 (2016). 10.1242/dev.134809.

13. Wu, R. S. et al. A rapid method for directed gene knockout for screening in G0 zebrafish. *Dev. Cell* **46**, 112–125 (2018). 10.1016/j.devcel.2018.06.003.

14. Hoshijima, K., Jurynec, M. J. & Grunwald, D. J. Precise editing of the zebrafish genome made simple and efficient. *Dev. Cell* **36**, 654–667 (2016). 10.1016/j.devcel.2016.02.015.

15. DiNapoli, S. E. et al. Synthetic CRISPR/Cas9 reagents facilitate genome editing and homology directed repair. *Nucleic Acids Res.* **48**, e38 (2020). 10.1093/nar/gkaa085.

16. Levic, D. S., Yamaguchi, N., Wang, S., Knaut, H. & Bagnat, M. Knock-in tagging in zebrafish facilitated by insertion into non-coding regions. *Development* **148**, dev199994 (2021). 10.1242/dev.199994.

17. Anzalone, A. V. et al. Search-and-replace genome editing without double-strand breaks or donor DNA. *Nature* **576**, 149–157 (2019). 10.1038/s41586-019-1711-4.

18. Petri, K. et al. CRISPR prime editing with ribonucleoprotein complexes in zebrafish and primary human cells. *Nat. Biotechnol.* **40**, 189–193 (2022). 10.1038/s41587-021-00901-y.

19. Davis, J. R. et al. Efficient prime editing in mouse brain, liver and heart with dual AAVs. *Nat. Biotechnol.* **42**, 253–264 (2024). 10.1038/s41587-023-01758-z.

20. Ely, Z. A. et al. A prime editor mouse to model a broad spectrum of somatic mutations in vivo. *Nat. Biotechnol.* **42**, 424–436 (2024). 10.1038/s41587-023-01783-y.

21. Adikusuma, F. et al. Optimized nickase- and nuclease-based prime editing in human and mouse cells. *Nucleic Acids Res.* **49**, 10785–10795 (2021). 10.1093/nar/gkab792.

22. Peterka, M. et al. Harnessing DSB repair to promote efficient homology-dependent and -independent prime editing. *Nat. Commun.* **13**, 1240 (2022). 10.1038/s41467-022-28771-1.

23. Li, X. et al. Development of a versatile nuclease prime editor with upgraded precision. *Nat. Commun.* **14**, 305 (2023). 10.1038/s41467-023-35870-0.

24. Kortüm, K. M. et al. Targeted sequencing of refractory myeloma reveals a high incidence of mutations in CRBN and Ras pathway genes. *Blood* **128**, 1226–1233 (2016). 10.1182/blood-2016-02-698092.

25. Ito, T. et al. Identification of a primary target of thalidomide teratogenicity. *Science* **327**, 1345–1350 (2010). 10.1126/science.1177319.

26. Donovan, K. A. et al. Thalidomide promotes degradation of SALL4, a transcription factor implicated in Duane Radial Ray syndrome. *eLife* **7**, e38430 (2018). 10.7554/eLife.38430.

27. Fink, E. C. et al. CrbnI391V is sufficient to confer in vivo sensitivity to thalidomide and its derivatives in mice. *Blood* **132**, 1535–1544 (2018). 10.1182/blood-2018-05-852798.

28. Zhang, W. et al. Enhancing CRISPR prime editing by reducing misfolded pegRNA interactions. *eLife* **12**, RP90948 (2024). 10.7554/eLife.90948.

29. van Bokhoven, H. et al. Mutation of the gene encoding the ROR2 tyrosine kinase causes autosomal recessive Robinow syndrome. *Nat. Genet.* **25**, 423–426 (2000). 10.1038/78113.

30. Afzal, A. R. et al. Recessive Robinow syndrome, allelic to dominant brachydactyly type B, is caused by mutation of ROR2. *Nat. Genet.* **25**, 419–422 (2000). 10.1038/78107.

31. Lima, A. R. et al. Phenotypic and mutational spectrum of ROR2-related Robinow syndrome. *Hum. Mutat.* **43**, 900–918 (2022). 10.1002/humu.24375.

32. Zhang, C., Brunt, L., Ono, Y., Rogers, S. & Scholpp, S. Cytoneme-mediated transport of active Wnt5b-Ror2 complexes in zebrafish. *Nature* **625**, 126–133 (2024). 10.1038/s41586-023-06850-7.

33. Mattes, B. et al. Wnt/PCP controls spreading of Wnt/β-catenin signals by cytonemes in vertebrates. *eLife* **7**, e36953 (2018). 10.7554/eLife.36953.

34. Brunt, L. et al. Vangl2 promotes the formation of long cytonemes to enable distant Wnt/β-catenin signaling. *Nat. Commun.* **12**, 2058 (2021). 10.1038/s41467-021-22393-9.

35. Bai, Y. et al. Ror2 receptor mediates Wnt11 ligand signaling and affects convergence and extension movements in zebrafish. *J. Biol. Chem.* **289**, 20664–20676 (2014). 10.1074/jbc.M114.586099.

36. Dranow, D. B., Le Pabic, P. & Schilling, T. F. The non-canonical Wnt receptor Ror2 is required for cartilage cell polarity and morphogenesis of the craniofacial skeleton in zebrafish. *Development* **150**, dev201273 (2023). 10.1242/dev.201273.

37. Antoniou, P. et al. Modified pegRNAs mitigate scaffold-derived prime editing by-products. *Nat. Commun.* **16**, 3374 (2025). 10.1038/s41467-025-58653-1.

38. Elworthy, S., Hargrave, M., Knight, R., Mebus, K. & Ingham, P. W. Expression of multiple slow myosin heavy chain genes reveals a diversity of zebrafish slow twitch muscle fibres with differing requirements for Hedgehog and Prdm1 activity. *Development* **135**, 2115-2126 (2008). 10.1242/dev.015719.

39. Dang, C. V. & Lee, W. M. Identification of the human c-myc protein nuclear translocation signal. *Mol. Cell. Biol.* **8**, 4048–4054 (1988). 10.1128/mcb.8.10.4048-4054.1988.

40. Hodel, M. R., Corbett, A. H. & Hodel, A. E. Dissection of a nuclear localization signal. *J. Biol. Chem.* **276**, 1317–1325 (2001). 10.1074/jbc.M008522200.

41. Ray, M., Tang, R., Jiang, Z. & Rotello, V. M. Quantitative tracking of protein trafficking to the nucleus using cytosolic protein delivery by nanoparticle-stabilized nanocapsules. *Bioconjug. Chem.* **26**, 1004–1007 (2015). 10.1021/acs.bioconjchem.5b00141.

42. Kuroki-Kami, A. et al. Targeted gene knockin in zebrafish using the 28S rDNA-specific non-LTR-retrotransposon R2Ol. *Mob. DNA* **10**, 23 (2019). 10.1186/s13100-019-0167-2.

43. Lalonde, R. L. et al. pIGLET: Safe harbor landing sites for reproducible and efficient transgenesis in zebrafish. *Sci. Adv.* **10**, eadn6603 (2024). 10.1126/sciadv.adn6603.

44. Komor, A. C., Kim, Y. B., Packer, M. S., Zuris, J. A. & Liu, D. R. Programmable editing of a target base in genomic DNA without double-stranded DNA cleavage. *Nature* **533**, 420–424 (2016). 10.1038/nature17946.

45. Gaudelli, N. M. et al. Programmable base editing of A•T to G•C in genomic DNA without DNA cleavage. *Nature* **551**, 464–471 (2017). 10.1038/nature24644.

46. Zhang, Y. et al. Programmable base editing of zebrafish genome using a modified CRISPR-Cas9 system. *Nat. Commun.* **8**, 118 (2017). 10.1038/s41467-017-00175-6.

47. Rees, H. A. et al. Improving the DNA specificity and applicability of base editing through protein engineering and protein delivery. *Nat. Commun.* **8**, 15790 (2017). 10.1038/ncomms15790.

48. Zhao, Y., Shang, D., Ying, R., Cheng, H. & Zhou, R. An optimized base editor with efficient C-to-T base editing in zebrafish. *BMC Biol.* **18**, 190 (2020). 10.1186/s12915-020-00923-z.

49. Rosello, M. et al. Precise base editing for the in vivo study of developmental signaling and human pathologies in zebrafish. *eLife* **10**, e65552 (2021). 10.7554/eLife.65552.

50. Qin, W. et al. ABE-ultramax for high-efficiency biallelic adenine base editing in zebrafish. *Nat. Commun.* **15**, 5613 (2024). 10.1038/s41467-024-49943-1.

51. Zhang, Y. et al. Cytosine base editors with increased PAM and deaminase motif flexibility for gene editing in zebrafish. *Nat. Commun.* **15**, 9526 (2024). 10.1038/s41467-024-53735-y.

52. Kim-Yip, R. P. et al. Efficient prime editing in two-cell mouse embryos using PEmbryo. *Nat. Biotechnol.* **42**, 1822–1830 (2024). 10.1038/s41587-023-02106-x.

53. Salem, A. R. et al. Prime editing in mice with an engineered pegRNA. *Vascul. Pharmacol.* **154**, 107269 (2024). 10.1016/j.vph.2023.107269.

54. Ben-Shachar, S. et al. Dominant versus recessive traits conveyed by allelic mutations - to what extent is nonsense-mediated decay involved? *Clin. Genet.* **75**, 394–400 (2009). 10.1111/j.1399-0004.2008.01114.x.

55. Wittkopp, N. et al. Nonsense-mediated mRNA decay effectors are essential for zebrafish embryonic development and survival. *Mol. Cell. Biol.* **29**, 3517–3528 (2009). 10.1128/MCB.00177-09.

56. Lai, S. et al. Effect of nonsense-mediated mRNA decay factor SMG9 deficiency on premature aging in zebrafish. *Commun. Biol.* **7**, 654 (2024). 10.1038/s42003-024-06356-6.

57. Koeppel, J. et al. Prediction of prime editing insertion efficiencies using sequence features and DNA repair determinants. *Nat. Biotechnol.* **41**, 1446–1456 (2023). 10.1038/s41587-023-01678-y.

58. Chen, P. J. et al. Enhanced prime editing systems by manipulating cellular determinants of editing outcomes. *Cell* **184**, 5635–5652.e29 (2021). 10.1016/j.cell.2021.09.018.

59. Ferreira da Silva, J. et al. Prime editing efficiency and fidelity are enhanced in the absence of mismatch repair. *Nat. Commun.* **13**, 760 (2022). 10.1038/s41467-022-28442-1.

60. Nelson, J. W. et al. Engineered pegRNAs improve prime editing efficiency. *Nat. Biotechnol.* **40**, 402–410 (2022). 10.1038/s41587-021-01039-7.

61. Ponnienselvan, K. et al. Reducing the inherent auto-inhibitory interaction within the pegRNA enhances prime editing efficiency. *Nucleic Acids Res.* **51**, 6966–6980 (2023). 10.1093/nar/gkad456.

62. Yan, J. et al. Improving prime editing with an endogenous small RNA-binding protein. *Nature* **628**, 639–647 (2024). 10.1038/s41586-024-07259-6.

63. Kosicki, M., Tomberg, K. & Bradley, A. Repair of double-strand breaks induced by CRISPR-Cas9 leads to large deletions and complex rearrangements. *Nat. Biotechnol.* **36**, 765–771 (2018). 10.1038/nbt.4192.

64. Adikusuma, F. et al. Large deletions induced by Cas9 cleavage. *Nature* **560**, E8–E9 (2018). 10.1038/s41586-018-0380-z.

65. Leibowitz, M. L. et al. Chromothripsis as an on-target consequence of CRISPR-Cas9 genome editing. *Nat. Genet.* **53**, 895–905 (2021). 10.1038/s41588-021-00838-7.

66. Paull, G. C. et al. Variability in measures of reproductive success in laboratory-kept colonies of zebrafish and implications for studies addressing population-level effects of environmental chemicals. *Aquat. Toxicol.* **87**, 115–126 (2008). 10.1016/j.aquatox.2008.01.008.

67. Meeker, N. D., Hutchinson, S. A., Ho, L. & Trede, N. S. Method for isolation of PCR-ready genomic DNA from zebrafish tissues. *Biotechniques* **43**, 610–614 (2007). 10.2144/000112619.

68. Clement, K. et al. CRISPResso2 provides accurate and rapid genome editing sequence analysis. *Nat. Biotechnol.* **37**, 224–226 (2019). 10.1038/s41587-019-0032-3.

Figure legends

Fig. 1 Prime editing substitution in the zebrafish *crbn* gene, comparing Cas9-nickase-based and nuclease-based Prime Editors. a, Schematic illustration of the functioning of prime editing by the Cas9-nickase-based Prime Editor (PE2) and the nuclease-based Prime Editor (PEn). b-d, Comparison between PEn and PE2 in prime editing substitution in the *crbn* gene with the pegRNA refolding procedure. Proportions of editing outcomes in individual injected embryos are shown by amplicon sequencing (b), alongside quantitative analyses of precise prime edits (c) and indels (d) comparing experimental conditions (n = 10 per group). P-values were determined using one-way ANOVA with Tukey's multiple comparison test in (c), and the Kruskal-Wallis test with Dunn's multiple comparison test in (d). Error bars in the bar graphs represent the mean and standard deviation, and individual data points indicate values from single injected embryos.

Fig. 2 Prime editing insertion in zebrafish *ror2* gene using Cas9-nuclease-based Prime Editor. a, Schematic illustration of the functional domains in the Ror2 protein and alignment of partial amino acid sequences within the tyrosine kinase domain. Sequences from multiple species, including those related to Robinow syndrome (RS) in humans W720X and the corresponding zebrafish W722X mutant, are aligned. The conserved tyrosine residue is highlighted. b, Schematic illustration of guide RNA (gRNA) designs for prime editing insertion in *ror2*. c, Schematic illustration of prime editing insertion by Cas9-nuclease-based Prime Editor (PEn). An additional DNA fragment, reverse-transcribed at the target cleavage site, containing the programmed insertion, is integrated into the genome via homology-directed repair or non-homologous end joining. d, Agarose gel images of genomic PCR products from embryos injected with Prime Editor mRNA and pegRNA/springRNA. PCR products of the *ror2* target region (top) and those after digestion with T7 endonuclease I (T7E1, bottom). e, Sequence alignment of the edits in the *ror2* target site obtained from embryos injected with PEn/springRNA. Prime editing insertion (TGA) is outlined, and the gRNA target sequence is underlined. f, Quantitative comparison of editing outcomes using different combinations of Prime Editor and gRNA. The proportion of sequence reads with each type of edit in amplicon sequencing is presented.

Fig. 3 Comparing different prime editing approaches in zebrafish embryos. a-c, Comparison between PEn and PE2 in prime editing insertion into *ror2* with various delivery methods. The proportion of editing outcomes in individual injected embryos was assessed through amplicon sequencing (a), along with a quantitative analysis of precise prime edit (b) and indels (c) across experimental conditions (n = 10 per group). d, Sequence alignment of edits in prime editing insertion in *ror2* via the PEn mRNA/springRNA combination. e, Schematic illustration of springRNA design featuring an abasic RNA spacer for prime editing insertion in *ror2*. f and g, Proportion of reads with scaffold incorporation (f) and precise prime edit (g) as determined by amplicon sequencing of prime editing insertion in *ror2* using control and abasic springRNA (n = 10 per group; one sample of the PEn RNP/abasic springRNA combination was excluded from analysis due to low read count). h and i, Prime editing insertion in the *adgrf3b* gene using PEn. The proportion of reads with a precise 3 bp (h) and 12 bp insertion (i) was evaluated using pegRNA or springRNA (n = 10 per group). P-values were determined by Welch's one-way ANOVA with Dunnett T3 multiple comparison test in b and c, and Kruskal-Wallis test with Dunn's multiple comparison test in f and g. Error bars in bar graphs represent the mean and standard deviation, and each individual data point indicates the value from a single injected embryo.

Fig. 4 Generation and characterisation of stable *ror2*^{W722X} mutant. a, Summary of the screening of F1 embryos. Sixteen embryos were genotyped per F0 founder. Each circle represents the genotype of a single embryo. The embryos were obtained by outcrossing the injected founder with wild-type fish; thus, all embryos with the mutation are heterozygous. b-d, Lateral images of wild type (b), zygotic *ror2*^{W722X} mutant (c), and maternal-zygotic (MZ) *ror2*^{W722X} mutant (d) larvae at 5 days post-fertilisation (dpf). e, Sanger sequencing chromatogram of wild type (top) and *ror2*^{W722X} mutant (bottom) at the prime editing target site in ror2. Prime editing insertion (TGA) is highlighted. The target sequence of the guide RNA is underlined, and the cleavage site of Cas9 is indicated by a dotted line. f, Quantitative analysis of total length comparing wild type, zygotic *ror2*^{W722X} mutant, and MZ *ror2*^{W722X} mutant at 5 dpf. Each data point on the graph represents the value from a single larva (n = 10 per group). P-values were determined by one-way ANOVA with a Tukey multiple comparisons test. Error bars represent the mean and standard deviation.

Fig. 5 Prime editing to insert a nuclear localisation signal sequence into the *smyhc1:gfp* transgene. a, Schematic representation of the prime editing insertion of the nuclear localisation signal (NLS) sequence into the *smyhc1:gfp* transgene and the expected eGFP expression in slow-twitch muscle fibres. b, Confocal microscopy image of the trunk muscle in *smyhc1:gfp* larvae at 4 days post-fertilisation (dpf) that were injected with the PEn RNP complex for the prime editing NLS insertion. Putative nuclear GFP expression is indicated by an arrowhead. Anterior is positioned to the left. c, Quantitative analysis of the efficiency of precise NLS insertion via amplicon sequencing. Two pegRNAs of differing lengths are compared (n = 10 per group, with one sample excluded from the analysis due to low read count). The p-value was determined using the Mann-Whitney U test. Error bars represent the mean and standard deviation, while individual data points on the graph indicate values from single injected larvae. d, Confocal microscopy images of the trunk muscle of F1 larvae exhibiting nuclear GFP expression at 2 dpf, obtained from founder 1 (see panel f). The GFP fluorescence channel (left) and pseudo-colour (right) images are shown. Anterior is to the left. e, Sequence alignment of the edits in the target site obtained from F1 embryos exhibiting nuclear GFP expression (founder 1). The NLS sequence is outlined in red. f, Summary of F1 embryo screening. F1 embryos obtained from 6 founders are categorised based on the GFP expression pattern. The embryos were produced by outcrossing the heterozygous *smyhc1:gfp* founder injected with the PEn RNP complex to wild type; thus, half of the embryos are expected to be negative for the *smyhc1:gfp* transgene.

Supplementary Figure legends

Supplementary Fig. 1 Prime editing substitution in the zebrafish *crbn* gene. a, Schematic illustration of the strategy for prime editing substitution in *crbn* gene. The nucleotides for substitution are indicated in red. The guide RNA (gRNA) target sequence is underlined. b, Quantitative analyses of precision scores comparing between PEn and PE2 in prime editing substitution in the *crbn* gene with the pegRNA refolding procedure (n = 10 per group). P-values were determined using Welch's one-way ANOVA with Dunnett T3 multiple comparison test. Error bars in the bar graphs represent the mean and standard deviation, and individual data points indicate values from single injected embryos.

Supplementary Fig. 2 Analysis of prime editing insertion in zebrafish *ror2* gene by sequencing the clones. a, Sequence alignment of the edits in the *ror2* target site obtained from 20 randomly selected bacterial clones comparing prime editing outcomes using PE2/pegRNA (top) and PEn/pegRNA (bottom) combinations. The guide RNA (gRNA) target sequence is indicated by green arrows. b, Quantitative comparison of editing outcomes using different combinations of Prime Editor and guide RNA. The proportion of the clones with each type of edit is presented.

Supplementary Fig. 3 Amplicon sequencing analysis of prime editing insertion in zebrafish *ror2* and *agdrf3b* genes. a-c, Quantitative analyses of precision scores comparing various experimental conditions for prime editing insertion in *ror2* gene using pegRNA (a) and springRNA (b), and in *adgrf3b* gene (c). The sample size is n = 10 per group and one sample of the PEn RNP/abasic springRNA combination was excluded from analysis in b due to low read count. P-values were determined by Welch's one-way ANOVA with Dunnett T3 multiple comparison test in a, and Kruskal-Wallis test with Dunn's multiple comparison test in b and c. Error bars in bar graphs represent the mean and standard deviation, and each individual data point indicates the value from a single injected embryo. d, Sequence alignment of edits in prime editing insertion in *ror2* via the PE2 mRNA/pegRNA (top) and PEn mRNA/pegRNA (bottom) combinations.

Supplementary Fig. 4 Prime editing insertion of a nuclear localisation signal sequence into the *smyhc1:gfp* transgene. a, The expression of *smyhc1:gfp* transgene in 2 days post-fertilisation (dpf) larvae. Lateral images of whole larvae (left) and the trunk muscle (right). Anterior is to the left. b, Confocal microscopy images of the trunk muscle of F1 larvae exhibiting nuclear GFP expression at 2 dpf, obtained from founder 2, 3, and 4 (see Fig. 5f). c, Sequence alignment of the edits in the target site obtained from F1 embryos exhibiting nuclear GFP expression (founder 2, 3, and 4). The nuclear localisation signal (NLS) sequences are outlined in red.

Figure 1

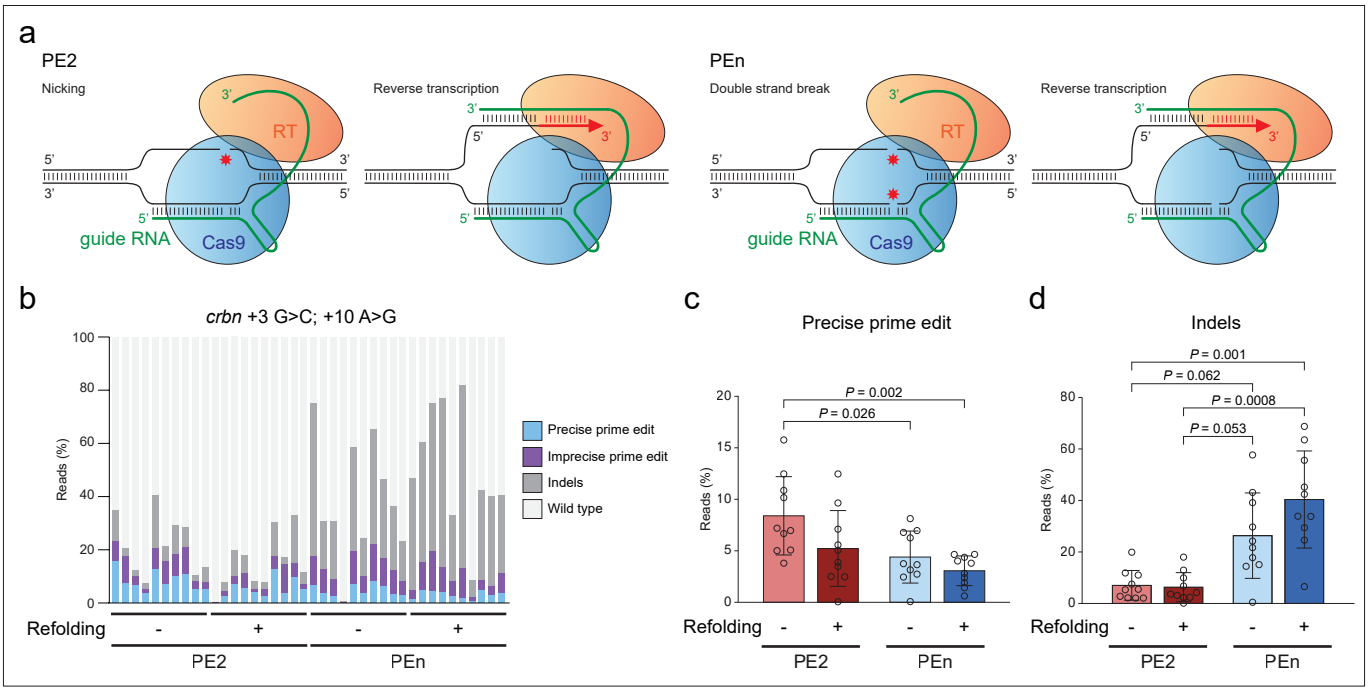
a
PE2
Nicking
Reverse transcription
PEn
Double strand break
Reverse transcription
RT
guide RNA
Cas9
3'
5'
b
crbn +3 G>C; +10 A>G
Reads (%)
Precise prime edit
Imprecise prime edit
Indels
Wild type
Refolding
PE2
PEn
c
Precise prime edit
P = 0.002
P = 0.026
d
Indels
P = 0.001
P = 0.062
P = 0.0008
P = 0.053

Figure 2

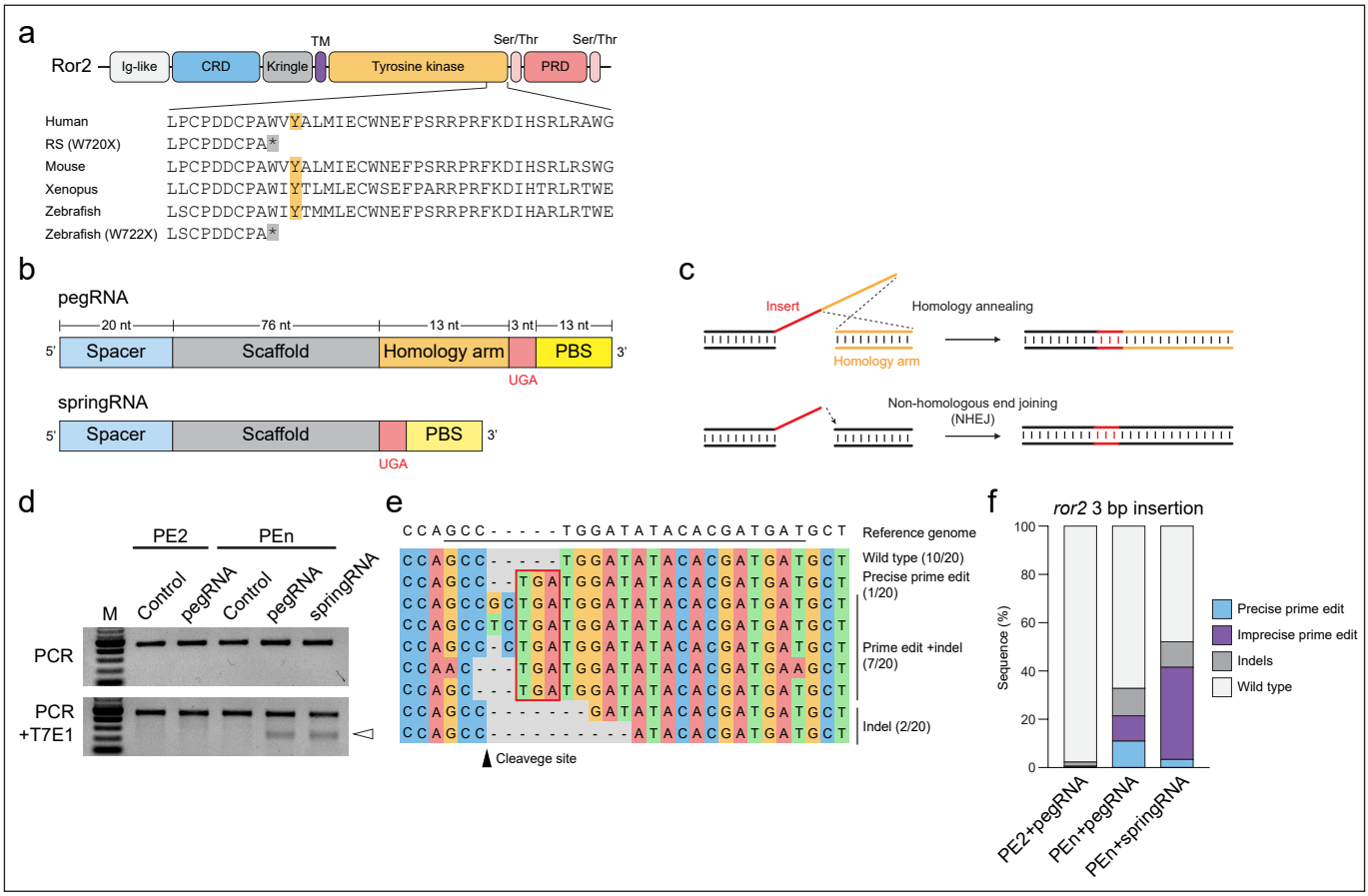
a
Ror2
Ig-like
CRD
Kringle
TM
Tyrosine kinase
Ser/Thr
Ser/Thr
PRD
Human LPCPDDCPAWVYALMIECWNEFPSRRPRFKDIHSRLRAWG
RS (W720X) LPCPDDCPA*
Mouse LPCPDDCPAWVYALMIECWNEFPSRRPRFKDIHSRLRSWG
Xenopus LLCPDDCPAWIYTLMLECWSEFPARRPRFKDIHTRLRTWE
Zebrafish LSCPDDCPAWIYTMMLECWNEFPSRRPRFKDIHARLRTWE
Zebrafish (W722X) LSCPDDCPA*
b
pegRNA
20 nt
76 nt
13 nt
3 nt
13 nt
5'
Spacer
Scaffold
Homology arm
PBS
3'
UGA
springRNA
5'
Spacer
Scaffold
PBS
3'
UGA
c
Insert
Homology annealing
Homology arm
Non-homologous end joining
(NHEJ)
d
PE2
PEn
M
Control
pegRNA
Control
pegRNA
springRNA
PCR
PCR
+T7E1
e
CCAGCC-----TGGATATACACGATGATGCT Reference genome
CCAGCC-----TGGATATACACGATGATGCT Wild type (10/20)
CCAGCC--TGATGGATATACACGATGATGCT Precise prime edit (1/20)
CCAGCCGCTGATGGATATACACGATGATGCT
CCAGCCTCTGATGGATATACACGATGATGCT
CCAGCC-CTGATGGATATACACGATGATGCT Prime edit +indel (7/20)
CCAAC---TGATGGATATACACGATGAAGCT
CCAGC---TGATGGATATACACGATGATGCT
CCAGCC-------GATATACACGATGATGCT Indel (2/20)
CCAGCC----------ATACACGATGATGCT
Cleavege site
f
ror2 3 bp insertion
Sequence (%)
100
80
60
40
20
0
PE2+pegRNA
PEn+pegRNA
PEn+springRNA
Precise prime edit
Imprecise prime edit
Indels
Wild type

Figure 3

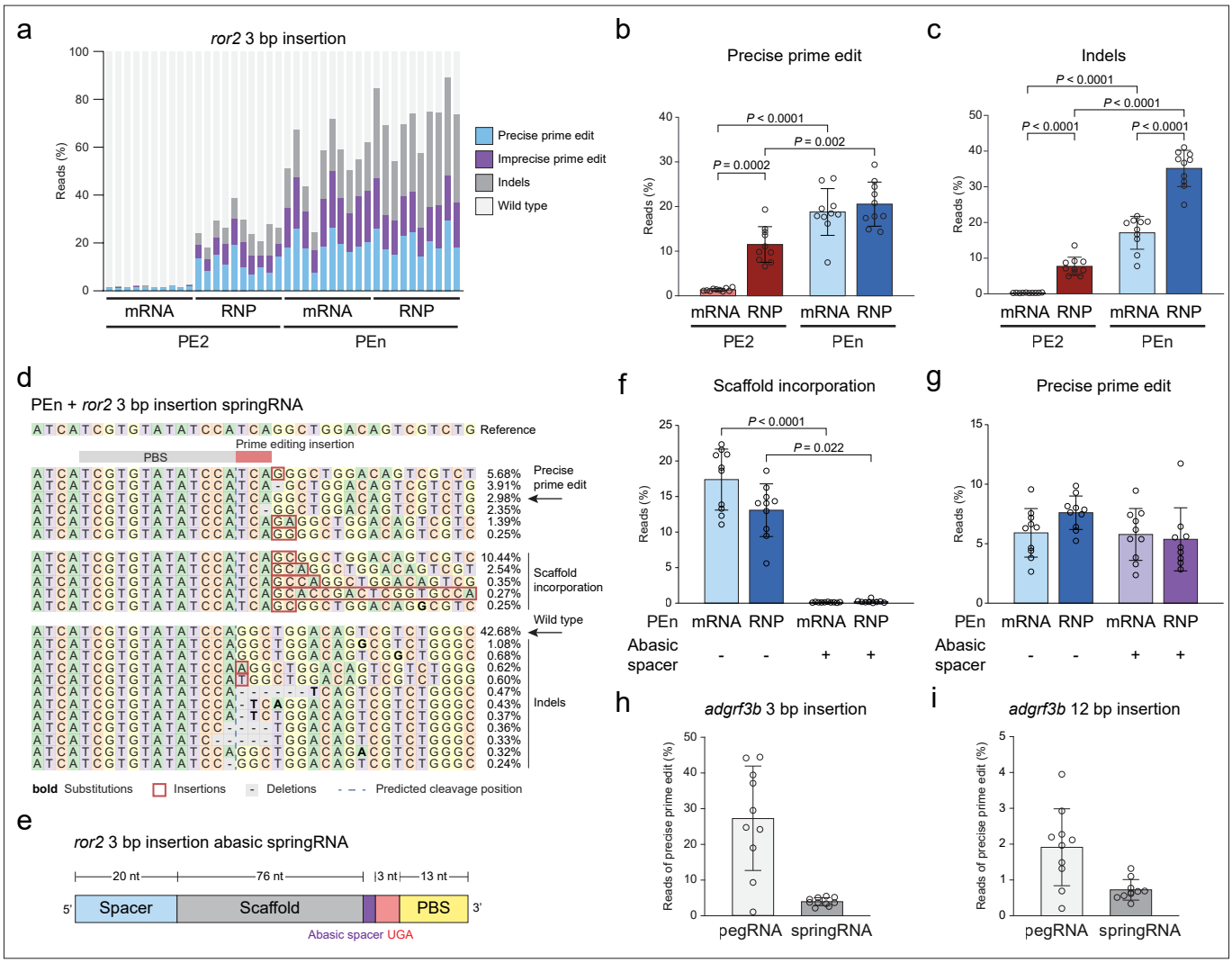
a
ror2 3 bp insertion
Reads (%)
Precise prime edit
Imprecise prime edit
Indels
Wild type
mRNA
RNP
mRNA
RNP
PE2
PEn
b
Precise prime edit
P < 0.0001
P = 0.002
P = 0.0002
Reads (%)
mRNA RNP mRNA RNP
PE2
PEn
c
Indels
P < 0.0001
P < 0.0001
P < 0.0001
P < 0.0001
Reads (%)
mRNA RNP mRNA RNP
PE2
PEn
d
PEn + ror2 3 bp insertion springRNA
ATCATCGTGTATATCCATCAGGCTGGACAGTCGTCTG Reference
Prime editing insertion
PBS
Precise prime edit
Scaffold incorporation
Wild type
Indels
bold Substitutions
Insertions
Deletions
Predicted cleavage position
e
ror2 3 bp insertion abasic springRNA
20 nt
76 nt
3 nt
13 nt
5'
Spacer
Scaffold
PBS
3'
Abasic spacer UGA
f
Scaffold incorporation
P < 0.0001
P = 0.022
Reads (%)
PEn mRNA RNP mRNA RNP
Abasic spacer - - + +
g
Precise prime edit
Reads (%)
PEn mRNA RNP mRNA RNP
Abasic spacer - - + +
h
adgrf3b 3 bp insertion
Reads of precise prime edit (%)
pegRNA springRNA
i
adgrf3b 12 bp insertion
Reads of precise prime edit (%)
pegRNA springRNA

Figure 4

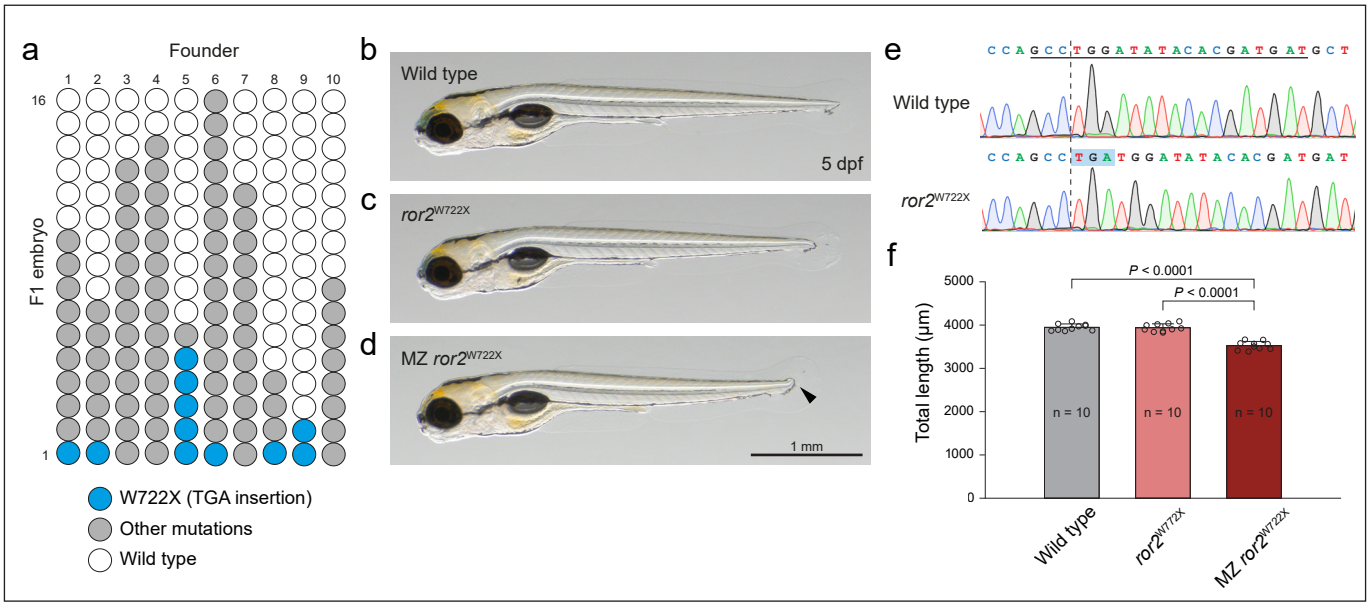
a
Founder
1 2 3 4 5 6 7 8 9 10
16
1
F1 embryo
W722X (TGA insertion)
Other mutations
Wild type
b
Wild type
5 dpf
c
ror2W722X
d
MZ ror2W722X
1 mm
e
Wild type
ror2W722X
f
P < 0.0001
P < 0.0001
Total length (µm)
5000
4000
3000
2000
1000
0
n = 10
n = 10
n = 10
Wild type
ror2W722X
MZ ror2W722X

Figure 5

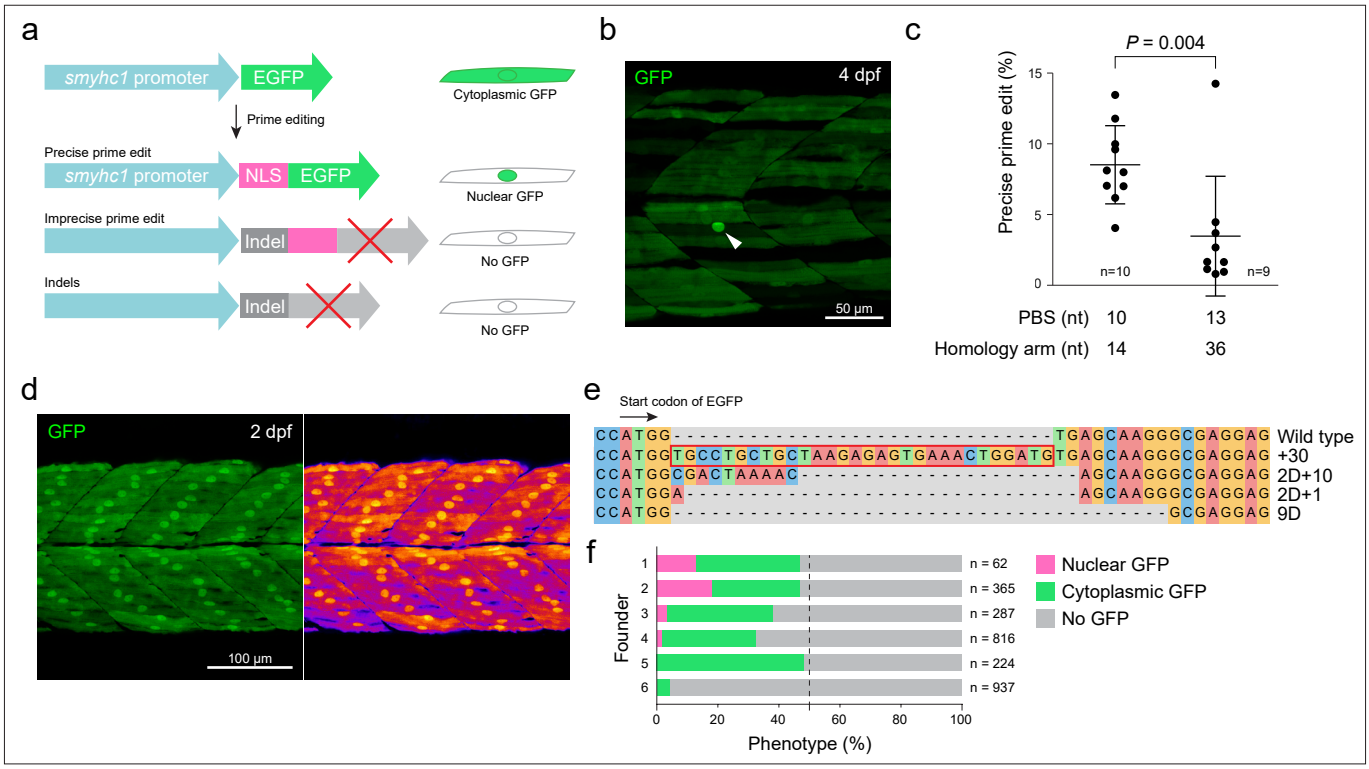
a
smyhc1 promoter
EGFP
Prime editing
Precise prime edit
smyhc1 promoter
NLS
EGFP
Imprecise prime edit
Indel
Indels
Indel
Cytoplasmic GFP
Nuclear GFP
No GFP
No GFP
b
GFP
4 dpf
50 µm
c
P = 0.004
Precise prime edit (%)
15
10
5
0
n=10
n=9
PBS (nt) 10 13
Homology arm (nt) 14 36
d
GFP
2 dpf
100 µm
e
Start codon of EGFP
CCATGG----------TGAGCAAGGGCGAGGAG Wild type
CCATGGTGCCTGCTGCTAAGAGAGTGAAACTGGATGTGAGCAAGGGCGAGGAG +30
CCATGGCGACTAAAAC----------AGCAAGGGCGAGGAG 2D+10
CCATGGA----------AGCAAGGGCGAGGAG 2D+1
CCATGG----------GCGAGGAG 9D
f
Founder
1
2
3
4
5
6
n = 62
n = 365
n = 287
n = 816
n = 224
n = 937
0
20
40
60
80
100
Phenotype (%)
Nuclear GFP
Cytoplasmic GFP
No GFP